

## DENSITY FUNCTION THEORY OF ELASTIC AND THERMAL PROPERTIES FOR CuTlSe<sub>2</sub> CRYSTAL

Y. J. DONG<sup>a,b\*</sup>, Y. L. GAO<sup>a</sup>

<sup>a</sup>*School of Science and Technology of Xinyang University, Henan Xinyang, 464000, China*

<sup>b</sup>*Institute of Atomic and Molecular Physics of Sichuan University, Sichuan, Chengdu, 610065, China*

In this paper, we focus on the study of the elastic and thermal properties of chalcopyrite structure of CuTlSe<sub>2</sub> crystal using the first principle theory. The lattice constants  $a$  and  $c$  are calculated which are excellent consistent with the earlier experimental and theoretical values. For the first time, it calculated and analysed the dependence of bulk modulus ( $B$ ) on temperature up to 1000K and on various pressure up to 20GPa. The thermal properties of the CuTlSe<sub>2</sub> crystal such as Debye temperature, the thermal expansion coefficient, the heat capacity  $C_v$  and  $C_p$  are also worked out by the quasi-harmonic Debye model. Most of the parameters are first reported.

(Received October 7, 2016; Accepted November 17, 2016)

*Keywords:* CuTlSe<sub>2</sub>; Density function theory; Elastic; Thermal

### 1. Introduction

The Cu-based semiconductors have particular advantages in all kinds of thin film solar cell material, which have great potential applications in the area of photovoltaic<sup>[1-4]</sup>. CuTlSe<sub>2</sub> belonging to the family of Cu-based chalcopyrites have the same structure with CuInSe<sub>2</sub>. Thus, more and more scholars began to study the properties of chalcopyrite materials by theoretical and experimental research. In the experimental studies, the electrical conduction in liquid CuTlSe<sub>2</sub> were reported by EIEIa<sup>[5]</sup>. In the same year, the electrical conductivity and thermal conductivity of the solid solution of CuTlSe<sub>2</sub><sup>[6]</sup> were investigated. And in the next year, they<sup>[7]</sup> measured the dielectric properties of CuTlSe<sub>2</sub> in the solid and liquid phases. Uemura<sup>[8]</sup> discussed the molten CuTlSe<sub>2</sub> by neutron diffraction measurements and found that there is a significant difference in bonding nature between Cu-Se and Tl-Se bonds. The chalcopyrite phase CuTlSe<sub>2</sub> is obtained by annealing the powder at 250°C for 1 hour by Abdel<sup>[9]</sup>. Although the CuTlSe<sub>2</sub> have been widely researched, rare theoretical studies were calculated the elastic and thermal properties for CuTlSe<sub>2</sub>.

The density functional theory (DFT) method has been established almost 40 years and successfully applied to the calculation of physical, chemical, biological and other aspects of materials. Especially for studying the structure and properties of semiconductor materials such as CuGaSe<sub>2</sub><sup>[10]</sup> and AgGaS<sub>2</sub><sup>[11]</sup>. Therefore it is worthwhile to present the elastic and thermal properties in CuTlSe<sub>2</sub> based on the density functional theory (DFT), in order to complete the experimental and theoretical work for these chalcopyrite compounds.

---

\* Corresponding author: dongyujing-001@163.com

## 2. Calculations method

In this paper, all the results of  $\text{CuTlSe}_2$  crystal were obtained by using a plane-wave basis set for the electronic wave functions and periodic boundary conditions. The exchange-correlation energy is evaluated in the generalized gradient approximation (GGA) Perdew-Burke-Ernzerhof (PBE) functional [12-15]. The calculations were performed following the BFGS procedure. The interaction between the valence electrons and the core-electrons is described by ultra-soft pseudopotentials. In order to satisfy the calculation accuracy and to ensure the calculation speed, the plane wave cut off energy is 350eV, and the whole Brillouin zone is calculated by the K point grid of  $4 \times 4 \times 4$ .

## 3. Result and discussion

### 3.1 structure and elastic properties

The most stable phase for  $\text{CuTlSe}_2$  is chalcopyrite (CH) structure(space group:  $\bar{1}42d$  122) which is belonging to tetragonal crystal system. The crystal structure of  $\text{CuTlSe}_2$  has been shown in Fig. 1. The existence of two different cations in every pure crystals results in two different interaction between Cu-Se and Tl-Se leading to two different bond lengths  $R_{\text{Cu-Se}}$  and  $R_{\text{Tl-Se}}$ . The tetragonal cell exhibits a distortion, defined by the parameter  $\eta = \frac{c}{2a}$ .

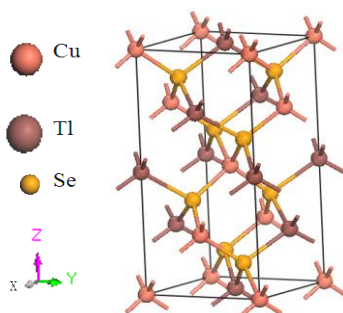


Fig 1. Crystal structure of  $\text{CuTlSe}_2$

In order to determine the structure parameters of  $\text{CuTlSe}_2$ , we first set up a series of lattice constants and calculate the corresponding volume of cell energy. Next step, we calculated the total energies as a function of volumes for  $\text{CuTlSe}_2$  and fitted them to the EOSs, as showed in Fig. 2. The data is fitted to Birch- Murnaghn<sup>[16]</sup> equation of state.

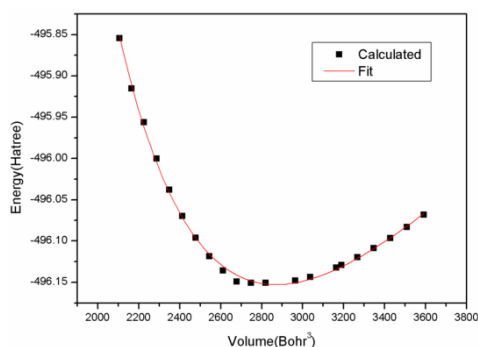


Fig 2. E-V curves of different lattice constant values

The lattice parameters, bulk modulus and its pressure derivative  $B'$  have been calculated and simulated by using GGA-PBE method. The fitted lattice parameters  $a$  and  $c$  are listed in table 1, which are close to the experimental works<sup>[17]</sup> than previous theoretical results<sup>[18, 19]</sup>. This results give us more confidence to study elastic properties and thermal properties further. The zero-pressure bulk modulus  $B$  and its pressure first derivative  $B'$  (table 1) have also been obtained by fitting of a Birch-Murnaghan EOS.

Table 1. Calculated lattice constants  $a$  (Å),  $c$  (Å), bulk modulus  $B$  (GPa) and its first derivative of  $\text{CuTiSe}_2$  compared to the available experimental and theoretical datas

	This work	Theory			Experiment
$a$ (Å)	5.92	5.83 <sup>a</sup>	5.829 <sup>b</sup>	6.041 <sup>c</sup>	5.832 <sup>d</sup>
$c$ (Å)	11.93	11.62 <sup>a</sup>	11.507 <sup>b</sup>	11.971 <sup>c</sup>	11.63 <sup>d</sup>
$B$	45.307	46.71 <sup>e</sup>			
$B'$	5.009				

a From Ref.[18]

b (LDA) From Ref. [19]. c (GGA) From Ref. [19]. d From Ref.[17] e (GGA)From Ref.[20]

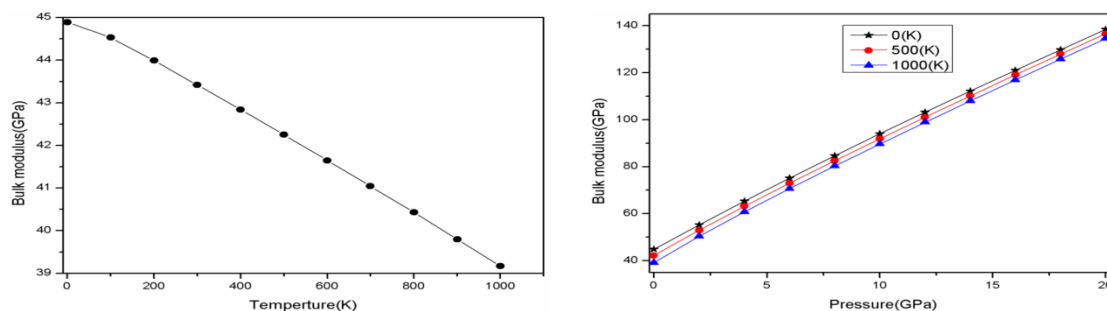


Fig. 3. The bulk modulus versus temperature(left) and pressure(right)

The bulk-modulus  $B$  as a function of temperature  $T$  has been investigated at zero-pressure, is plotted in Fig3(left). The relationship of them could be obtained by solving the equation<sup>[26]</sup>:  $\left(\frac{\partial G^*(V;p,T)}{\partial V}\right)_{p,T}$ . The bulk modulus  $B$  can be expressed as:

$$B_T(p,T) = -V \left( \frac{\partial p}{\partial T} \right)_T = V \left( \frac{\partial^2 G^*(V;p,T)}{\partial V^2} \right)_{p,T}$$

where  $G^*$  is the Gibbs function.  $V$  represents the volume. Following the Fig.3(left) we note that the bulk modulus  $B$  decreases drastically with increasing temperature in the 0~1000K range. The results means the cell volume have a sharp change. The third-order polynomial have been obtained by fitting the  $B$ - $T$  data points employing origin8.0 code. The equation is:

$$B = 44.92713 - 4.27 \times 10^{-3} T - 2.73427 \times 10^{-6} T^2 + 1.26263 \times 10^{-9} T^3$$

,for  $T < 1000\text{K}$ .

Fig. 3(right) displays the relationship between bulk modulus  $B$  and pressure  $P$  at different temperatures ( $T=0,500\text{K},1000\text{K}$ ). As the pressure goes higher, the bulk modulus have the same changing trend at the different temperature.

### 3.2 Thermal properties

We used the quasi-harmonic Debye model<sup>[27]</sup> to study more information about the thermal properties of  $\text{CuTiSe}_2$ . The ratio and heat capacity have been calculated at the different pressure ( $P$ )

and temperature( $T$ ) in the ranges of 0 ~ 20 GPa and 0~ 1000 K.

Fig.4 plots the relationships of the (relative volume) ratio  $V/V_0$  with temperature( $T$ ) and pressure( $P$ ), respectively. In Fig. 4 (left), the ratio  $V/V_0$  decreases slowly with the increasing of the temperature from 0 to 1000 K at different pressure  $P = 4, 8, 12, 16$  and 20 GPa. In Fig. 4 (right), it can be found that the ratio  $V/V_0$  decreases as the pressure changes from 0 to 20 GPa at different temperatures  $T = 0, 500,$  and 1000 K, respectively. The  $V/V_0$  decreases exponentially among different temperatures at low pressure. As the pressure increases, the  $V/V_0$  is close to linear decrease. In a word, the pressure have more significant influences on the  $V/V_0$  are much more than the temperature.

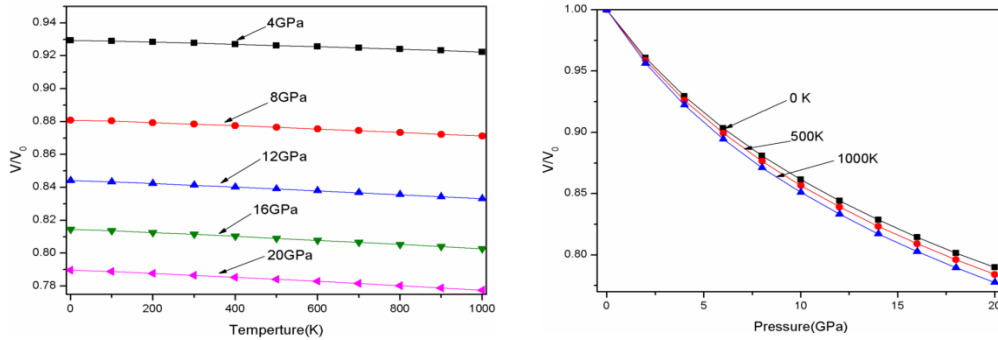


Fig. 4. The ratio  $V/V_0$ - $T$  (left) and  $V/V_0$ - $P$  (right) diagram of  $\text{CuTlSe}_2$

Fig. 5 shows the heat capacity  $C_v$  and  $C_p$  as a function of temperature under different pressures (0 and 20 GPa). We can see from Fig.5, under the same pressure, the heat capacity ( $C_v$  and  $C_p$ ) increases with the increase of temperature, in 0 ~ 500K of heat capacity with temperature increased significantly. The temperature is greater than 800K, the heat capacity  $C_v$  is close to a constant at sufficient high temperatures, obeying Dulong and Petit's Rule and approaching the Dulong-Petit limit. At 0 GPa and 300 K, the  $C_v$  and  $C_p$  are  $98.21 \text{ J mol}^{-1} \text{ K}^{-1}$  and  $99.86 \text{ J mol}^{-1} \text{ K}^{-1}$ , respectively.

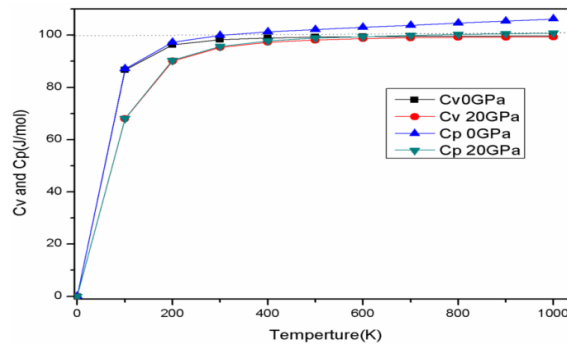


Fig. 5. Heat capacity of  $\text{CuTlSe}_2$  versus temperatures under different pressures

Fig.6 presents the temperature dependence of the Debye temperature  $\theta_D$  (k) and the expansion coefficient  $\alpha(10^{-5}/\text{K})$  for various pressure. Meanwhile,  $\alpha$  increases quickly as the temperature at a given pressure particularly at zero pressure below 200k. The various of Debye temperature  $\theta_D$  (k) as a function of pressure and temperature illustrated by our results is displayed in Fig6(right). As the pressure goes higher, the effect of change of the temperature on the Debye temperature values is not significant.

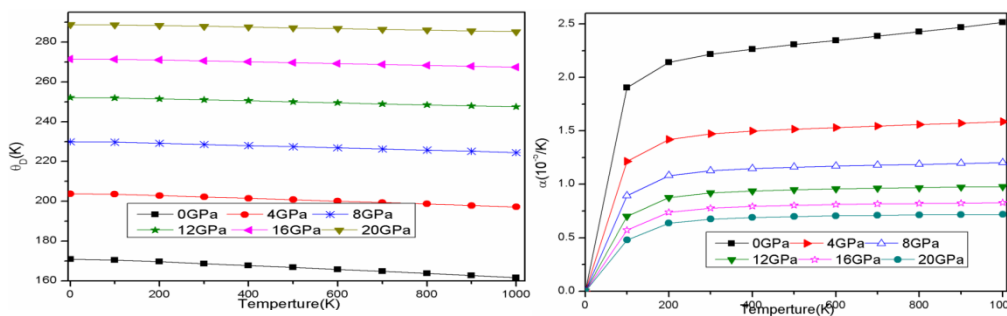


Fig 6. The Debye temperature (left) and the thermal expansion coefficient (right) of  $\text{CuTiSe}_2$  under different pressure

#### 4. Conclusions

The parameters of the basic properties of  $\text{CuTiSe}_2$  crystal have been calculated by using the plane wave pseudopotential density functional theory as well as quasi-harmonic Debye model. Firstly, the relationship between the energy and the volume change of  $\text{CuTiSe}_2$  (E-V) is calculated. And then, the elastic and thermal properties of  $\text{CuTiSe}_2$  at different temperatures and pressures are calculated. The lattice constants (a,c), the bulk modulus B and its derivative  $B'$  have been evaluated and compared with experimental data. Our results are in good agreement with the experimental data.

The pressure dependence of thermal parameters including heat capacity  $C_v$  and  $C_p$ , the Debye temperature  $\theta_D(k)$ , and the expansion coefficient  $\alpha(10^{-5}/K)$  are also investigated for the first time. The results indicated: at same temperature, the heat capacity ( $C_v$ ) decreased with the pressure increasing, while increase with temperature increasing under the same pressure. In addition, the heat capacity increased significantly with the temperature increasing in the range of 0 ~ 500K. The heat capacity is close to the classical limit of Dulong Petit's law when the temperature is higher than 800k.

#### Acknowledgements

This work was supported by the Key Scientific Research Project of Higher Education of Henan Province. (Grant No.: 15A140037, 16A140033).

#### References

- [1] J.L Shay, J.H Wernick. Oxford: Pergamon Press.(1975)
- [2] R.W Birkmire, E.Eser, Annu. Rev. Mater. Sci. **27**(1),625 (1997)
- [3] S.Wagner, J.L.Shay, P.Migliorato. App. Phys. Lett. **25**(8), 434 (2003)
- [4] M.AlonsoI.,K.Wakia,J.Pascual,M.Garriga,N.Yamamoto,PHYS.Rev.B **63**, 075203(2001)
- [5] A.H.Abou, ElEla,N.Abdelmohsen.Appl.Phys. **A26**,171 (1981)
- [6] A. H.Ela, Abou El, H. H. A. Labib, and N. Abdelmohsen. Physica Status Solidi . **67**, k43 (1981)
- [7] A.H.Abou,ElEla etal,Phys. stat. sol. **A69**,377 (1982)
- [8] O. Uemura, T. Akai, Y. Kameda, et al. Physica Status Solidi. **112**(2),467 (1989)
- [9] A.Abdel, J. Mater. Sci. Technol. **17**(2), 229 (2001)

- [10] C. Parlak, R. Eryiit, J. Phys. Cond. Matter. **73**(24), 1413 (2006),
- [11] M. G. Brik Phys. Status Solidi. **8**(9), 2582 (2011),:
- [12] P. P. John, B. Kieron, E. Matthias, Phys. Rev. Lett. **77**(18), 3865(1996)
- [13] L. Guo, G. Hu, W. J. Feng, S. T. Zhang, Acta Phys.-Chim. Sin. **29**(5), 929(2013)
- [14] J. H. Yuan, B. Gao, W. Wang, J. F. Wang, Acta Phys. Chim. Sin. **31**(7), 1302(2015)
- [15] C. Stampfl, C. G. Van-de-Walle, Phys Rev B **59**(8), 5521(1999)
- [16] F. Birch, Finite. Phys. Rev. **71**(11), 809(1947)
- [17] H. Hahn, G. Frank, W. Klingler, A. Meyer, and G. Storer. Z. Anorg. Chem. **271**, 153 (1953)
- [18] Voroshilov, Yu. V., Evstigneeva, T. L. Nekrasov, I. Ya., Kristallokhimicheskie tablitsy troinykh khal'kogenidov. [J]. (Crystal-Chemical Tables for Ternary Chalcogenides), Moscow: Nauka, (1989)
- [19] Y. Hinuma, F. Oba, K. Yu, Phys. Rev. B. **88**, 035305 (2013),
- [20] J. J. Liu, L. B. Shi, J. At. Mol. Phys. **4**, 672(2014)
- [21] D. R. Hamann, X. Wu, K. M. Rabe, Phys. Rev. B **71**, 035117 (2005),
- [22] M. Born, K. Huang, Dynamical Theory of Crystal Lattice (Oxford University Press, Oxford) (1954)
- [23] M. Von, Lehrbuch der kristallphysik, B. G. Teubner, (1928).
- [24] A. Reuss, Zamm-Journal of Applied Mathematics & Mechanics **9**(1), 49(1929)
- [25] R. Hill, Proc. Phys. Soc. London A . **65**, 349.(1952)
- [26] A. A. Maradudin, E. W. Montroll, G. H. Weiss. Theory of Lattice Dynamics i the Harmonic Approximation, 5,(1971)
- [27] M. A. Blanco, E. Francisco, V. Luaña, Computer Phys. Communications, **158**(1), 57 (2004)